Masonry Wall Interior Insulation Retrofit Embedded Beam Simulations

Kohta Ueno[1]

ABSTRACT

There is a large stock of uninsulated mass masonry buildings; the retrofit of insulation is commonly considered to improve their energy performance. Some durability issues associated with interior insulation have been or are being addressed, such as interstitial condensation and freeze-thaw damage issues.

However, another durability risk is the hygrothermal behavior of moisture-sensitive wood beams embedded in the load-bearing masonry. Interior insulation reduces the beam end temperatures, reduces available drying potential, and results in higher relative humidity conditions in the beam pocket: all of these factors pose a greater risk to durability.

Three-dimensional thermal simulations were performed to examine the effect of interior insulation on embedded wood members. Simulations were run for the cases both of large wood members ("beams") and smaller dimension lumber members ("joists"). In addition, simulations were run of various methods that would increase heat flow to the beam ends; the resulting effect on overall heat loss was also examined. This was followed by one-dimensional hygrothermal simulations to gain greater insight into the beam end behavior, including airflow effects.

Results indicate that the methods to increase beam end temperature have mixed results. Metal spreader plates increase the temperatures at smaller joists, but they do not appear to be a worthwhile strategy in larger beams. The thinning of insulation near the embedded beam ends appears to have minimal thermal effects. Hygrothermal simulations give results that vary strongly based on starting assumptions and material properties: field monitoring to determine in-situ conditions is recommended instead.

INTRODUCTION

There is a large stock of historic, uninsulated mass masonry buildings; the retrofit of insulation is commonly considered to improve their energy performance. Although exterior insulation retrofits provide ideal protection of the existing structure (Hutcheon 1964, Nady et al. 1997), they are incompatible with goal of the preservation of the historic exterior appearance. Therefore, interior insulation of these buildings has become increasingly common.

Some durability issues linked with previous insulation techniques have been or are being addressed, including interstitial condensation and brick freeze-thaw damage However, another durability risk that has received less investigation is the hygrothermal

[1] Kohta Ueno, Senior Associate, Building Science Corporation, Somerville, MA

behavior of moisture-sensitive wood beams embedded in the load-bearing masonry. With the retrofit of interior insulation, the embedded beam ends will spend longer periods at colder temperatures than their pre-retrofit condition. Therefore, these wood members will have reduced drying potential, and also be subjected to higher relative humidity (RH) conditions in the beam pocket: both of these factors pose a greater risk to durability.

Therefore, three-dimensional thermal simulations were performed to examine the effect of interior insulation on embedded wood members. Simulations were run for the cases both of large wood members ("beams") and smaller dimension lumber members ("joists"). In addition, simulations were run of various methods that would allow increased heat flow to the beam ends, including the use of passive (non-heated) metal "spreader" plates that bypass the insulation; use of less insulation at the beam pockets; and the elimination of insulation at the area surrounding the embedded member. The effect of these methods on overall heat loss through the opaque wall was also examined. The results of these thermal simulations were also used in conjunction with one-dimensional hygrothermal simulations to gain greater insight into the beam end behavior.

PREVIOUS WORK

Interior insulation of mass masonry wall assemblies in cold climates poses some specific challenges, including interstitial condensation of interior-sourced moisture (at the insulation-masonry interface), and risks of freeze-thaw damage to the exterior masonry. Literature on this practice spans back several decades. Rousseau and Maurenbrecher (1990) provide an overview of the issues faced when adapting existing massive masonry buildings for current use. The overview paper by Gonçalves (2003) gives best practice recommendations for retrofitting insulation to massive masonry structures, based on existing practice in the Montreal region. Like Rousseau and Maurenbrecher, he emphasizes controlling both exterior rain penetration, and air leakage and vapor diffusion from the interior. In addition, he recommends limiting thermal insulation, in order to limit the reduced temperatures at the masonry. The problems and solutions are also outlined by practitioners such as Maurenbrecher et al. (1998), and Straube and Schumacher (2002, 2004).

Masonry freeze-thaw issues (due to reduced outward heat flow and drying) have been examined by Mensinga et al. (2010) (among others). They suggest the use of material property testing (determination of critical degree of saturation, or S_{crit}) as an input to hygrothermal simulations, using a limit states design approach.

The embedded floor joist decay issue has been studied by several practitioners, including field monitoring and computer simulations.

Dumont et al. (2005) monitored moisture content of wood structural members embedded in masonry in two low-rise residences that were retrofitted with insulation in Wolseley, SK (DOE Zone 7, "dry" climate) and Kincardine, ON (DOE Zone 6A, "moist" climate). The Wolseley house was insulated with mineral wool, with a polyethylene

vapor barrier; the Kincardine house was insulated with spray polyurethane foam. The foam insulation encased the wood members where they were seated in the masonry wall. Data showed that the wood members of the Wolseley house remained at safe moisture content levels (10-15%) throughout the monitoring period. However, the Kincardine house showed consistently elevated moisture contents (20%+) at several locations. It was suspected that the moisture source was capillary uptake from the wet foundation, but rainwater absorption through the face of the masonry (due to surface detailing) was not eliminated as a possible source.

Scheffler (2009) examined the problem of interior retrofits of masonry structures, focusing on moisture problem at wooden beam ends. He used DELPHIN two-dimensional hygrothermal simulation software to examine the geometry of a wooden beam embedded in brick masonry under steady state conditions (23° F/-5° C/80% RH exterior; 68° F/20° C/50% RH interior; 90 days). These simulations indicated the moisture risks associated with insufficient control of airflow or moisture vapor flow (diffusion) from interior sources. This was followed by one-dimensional and two-dimensional simulations using transient weather data (Bremen; mild, maritime climate with high rain and humidity), indicating increases in relative humidity and liquid water (condensation) at the beam ends due to the addition of insulation.

Scheffler also described the historic methods to increase embedded beam longevity, such as charring the beam end to increase moisture resistance, and the addition of exterior-to-interior ventilation at the beam pocket. He discussed current methods to ameliorate these moisture issues due to insulation retrofits, including replacement of wood floor/ceiling assemblies with non-moisture sensitive materials (e.g., concrete), and possibly the addition of heat and/or ventilation at the wood beam end.

Morelli et al. (2010) collaborated with Scheffler, continuing examinations of this issue. They proposed the solution of leaving a gap in the insulation of 12” (300mm) above and below the floor, resulting in a 30” (770 mm) gap (12” gap×2 plus floor depth). Two- and three-dimensional heat transfer simulation showed that given the reduction of heat flow from the uninsulated to insulated cases (60% reduction), roughly 25% of the difference was “given back” due to the gap. This is equal to a 45% reduction in heat flow from the uninsulated case. This work was followed by two-dimensional DELPHIN hygrothermal simulations of the embedded beam (in a Bremen climate). Relative humidity levels in a corner of the beam pocket (and equilibrium wood moisture content) were compared between cases. The existing, uninsulated wall showed a drying trend, the fully insulated wall showed seasonal increases in RH, and the gapped insulation wall showed performance between the two previous cases (but with increasing moisture levels). However, these results assumed a relatively high wind-driven rain loading factor: switching to a lower loading factor, the gapped insulation assembly showed a general drying trend.

THERMAL SIMULATIONS

The first portion of the work was to run three-dimensional finite-element thermal simulations using HEAT3 v. 5.1 (Blomberg 1996), to examine the effect of interior

insulation on embedded wood members. Simulations were run for the cases both of large wood members ("beams") and smaller dimension lumber members ("joists").

The simulated "beam" case was a 12" x 8" (0.3 m x 0.2 m) beam embedded in an 18" (0.45 m) thick masonry to a depth of 8" (0.2 m). A 78" x 78" (2 m x 2 m) square section of wall was simulated; the associated wood flooring was also included. A 1" thick (25 mm) cast iron or steel bearing plate is commonly used to spread the beam loads on the masonry; it has the added benefit of acting as a capillary break. This element was explicitly modeled (shown in pink). Beams are often "fire cut," with the end angled inwards; this was not modeled. Note that these dimensions remain identical throughout these simulations; differences in images are due to aspect ratio shifts in the graphic.

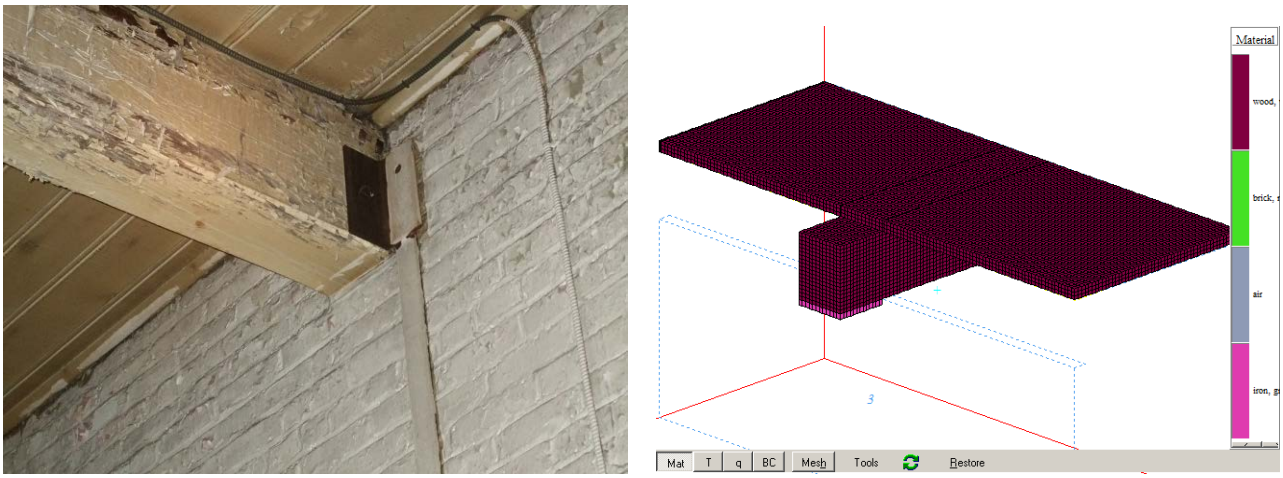

Figure 1: Typical embedded beam (left), and HEAT3 representation of beam, floor, & plate (right)

Interior temperature was fixed at 68° F (20° C), and exterior temperature at 7° F (-14° C), which is the Boston 99.6% design temperature. The interior heat transfer coefficient was modified at two-sided and three-sided corners, to account for the effect of reduced heat flow at these conditions.

The baseline uninsulated case is shown in Figure 2; beam end surfaces are range from 28 to 44° F (-2 to 6° C). The heat conduction through the bearing plate is clear from the asymmetric temperature ranges. Note that the coldest portions of the beam would actually not be present assuming a fire cut end. These simulations assume steady-state conditions, so no benefit from the thermal mass of the masonry is reflected here.

In addition, some early cases examined the effect of the air space that typically surrounds the beam in the pocket: a ~¼" (6 mm) gap was used. The beam end temperature regimes were close to identical in the air gap and non-air gap cases; this might be explained by the small size of the gap, and the relative thermal conductivities of air at 0.0043 Btu·in / (hr·ft^2·°F) or 0.03 W/m·K vs. wood at 0.0144 Btu·in / (hr·ft^2·°F) or 0.1 W/m·K. Note, however, that an air space has a significant effect in terms of capillary liquid water transport between the masonry and the wood.

This was followed by cases which added 2"/50 mm of foam insulation (R-12/RSI 2.1) to the interior surface of the masonry (Figure 2). The surface temperatures of the beam

end dropped to the 12-22°F (-5 to -11° C) range. These cold temperatures penetrate into the “core” of the beam; a temperature distribution at a horizontal section is shown in Figure 4.

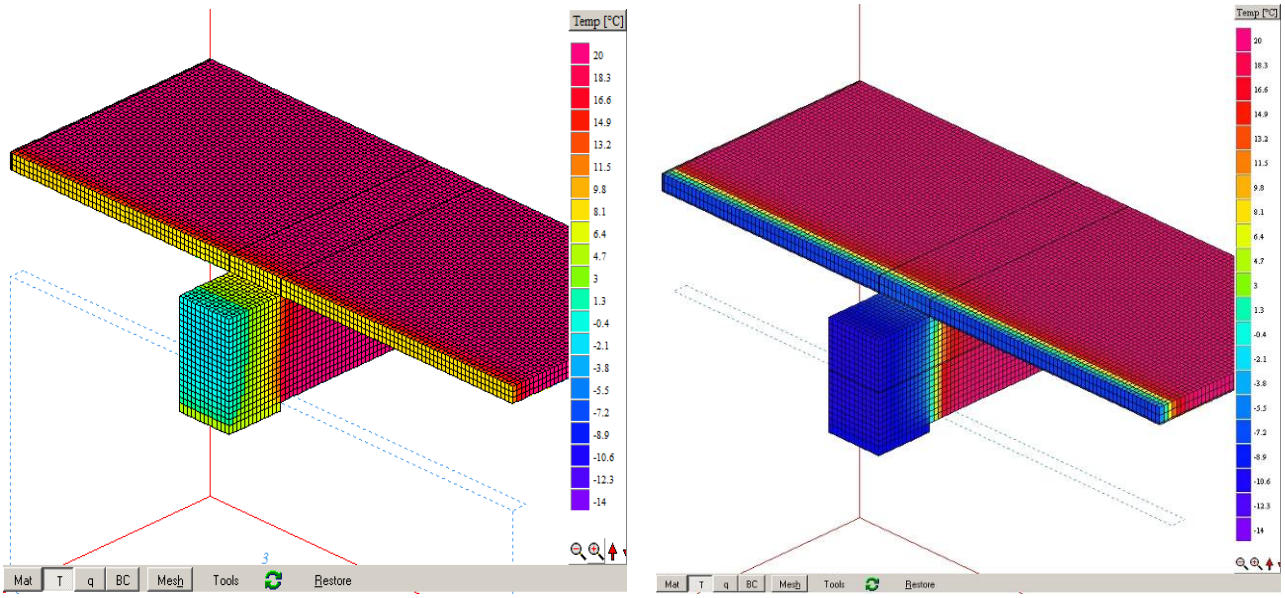

Figure 2: Embedded beam uninsulated case (left) and insulated case (right)

This was followed by simulations of methods to increase heat flow at the beam end, which increase the post-retrofit beam end temperature. One approach was to install thinner (1”/25 mm) thick foam in an area 16”/0.4 m around the beam; a minimum thickness was included to provide an air seal at the beam penetration. The resulting temperature distribution (Figure 3, left) seems largely identical to the original case.

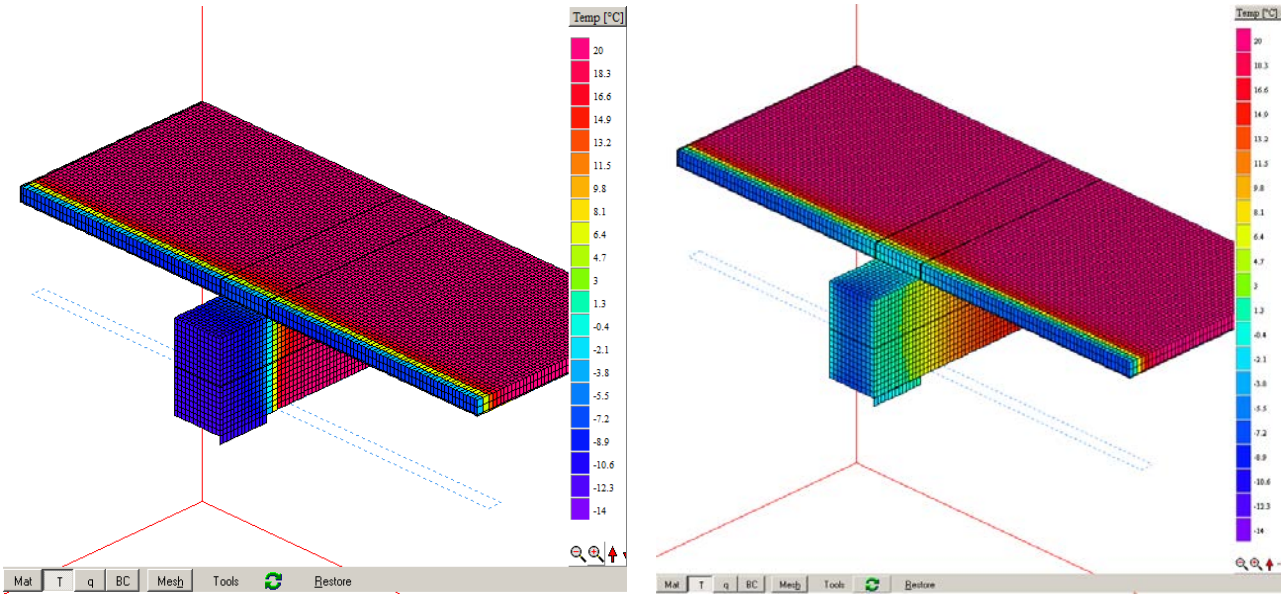

Figure 3: Thinned foam case (left) and 3 mm thick aluminum plates case (right)

Another option was to add metal plates to the sides of the beam, to bypass the insulation. After several iterations, a pair of 3 mm aluminum plates was selected; they extended to the full depth of the beam pocket, and had an exposed length of roughly 2 times the pocket depth on the interior. These were simulated as having full contact with the beam. The results in Figure 3 (right) show that the vertical faces of the beam are close to the original temperatures, but the middle of the beam is colder. This shows the limitation of the geometry of the problem: wood has a relatively high insulating value, thus making the nominal goal of "transmitting" heat laterally into the pocket more difficult.

These results are also shown in plan section in Figure 4, for the uninsulated, insulated, and "insulated with plates" cases. These images show that the plates definitely increase the beam temperatures through its thickness, although it is colder than the uninsulated case.

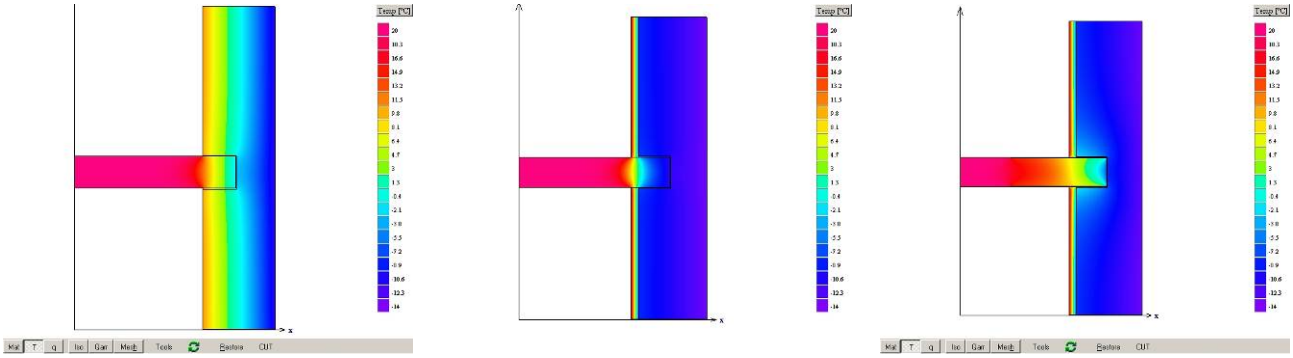

Figure 4: Beam cases horizontal section at mid height in beam: uninsulated (left), insulated (middle), and aluminum spreader plates (right)

However, there are several potential problems with the aluminum spreader plate solution: one is that there is increased risk of interior air leakage into the beam pocket, given the difficulty of forming an air seal around the plate adjacent to the beam. This could result in air-transported moisture from the interior, and condensation inside the beam pocket. Second, there is the potential risk of condensation of interior air on the cold exposed surfaces of the aluminum plates. The coldest surfaces temperatures of the interior exposed plate are in the range of 44-46° F (6-8° C); condensation would start at interior conditions of 70° F, 35-40% RH. If interior wintertime humidity conditions were well controlled, this would minimize condensation risks.

This work was followed by simulations of smaller members at a closer spacing, or "joists." These simulations used 2"x12" (0.5 m x 0.3 m) wood members at 16" (0.4 m) o.c. spacing. Similar to previous work, cases were run with uninsulated, insulated, and insulated with aluminum plate conditions (Figure 5). The aluminum plates made the beam end temperatures at least as warm as their pre-insulation condition. However, it is difficult to imagine the installation of these plates at a large number of closely spaced joists, as opposed to the more widely spaced beams.

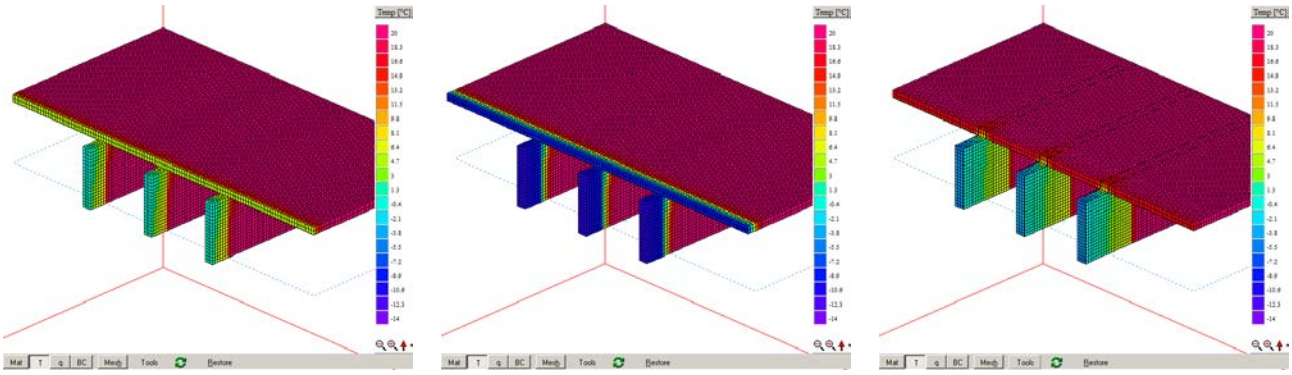

Figure 5: Joist cases: uninsulated (left), insulated (middle), and aluminum plates (right)

Therefore, several more possible options were run. One was to thin the foam to 1"/25 mm at the rim joist area, as per Figure 6 (left): similar to the analogous beam case, a negligible increase in beam end temperatures was observed. Another option was to omit the rim joist insulation entirely, similar to Morelli et al.'s (2010) work. The resulting temperatures are shown in Figure 6 (right), showing a temperature distribution close to the original, uninsulated case. However, without the addition of an air barrier at the beam pocket, there is a risk of interstitial condensation at the concealed masonry surface. Specifically, at design conditions (7° F/14° C), the beam pocket temperatures are in the 22 to 25° F (-4 to -6° C) range, which has condensation risks at 70° F/12% RH or higher. This condensation risk could not be addressed by controlling interior RH in an occupied building.

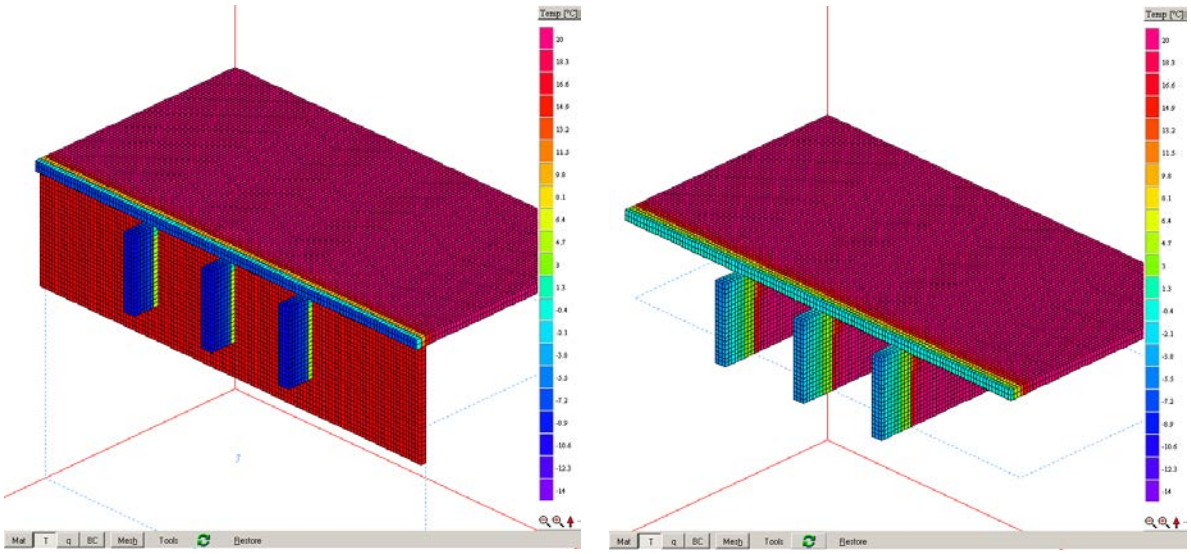

Figure 6: Joist cases: 1" (25 mm) thinned foam at floor joist area (left) and omitted band joist insulation (right)

The impact of these methods of increasing beam end temperatures on overall heat loss is shown in Figure 7. It compares the heat flux (for 42 sf/4 m^2 of wall assembly with joist framing, at Boston design conditions) for the uninsulated case, the insulated case, the use of aluminum plates, and the uninsulated band joist. The addition of insulation

results in an 80% reduction in heat flux. The addition of the aluminum plates result in the loss of 9% of those savings (i.e. 75% reduction from uninsulated). The use of an uninsulated rim joist space result in the loss of 20% of those savings being given up (i.e. 66% reduction from uninsulated).

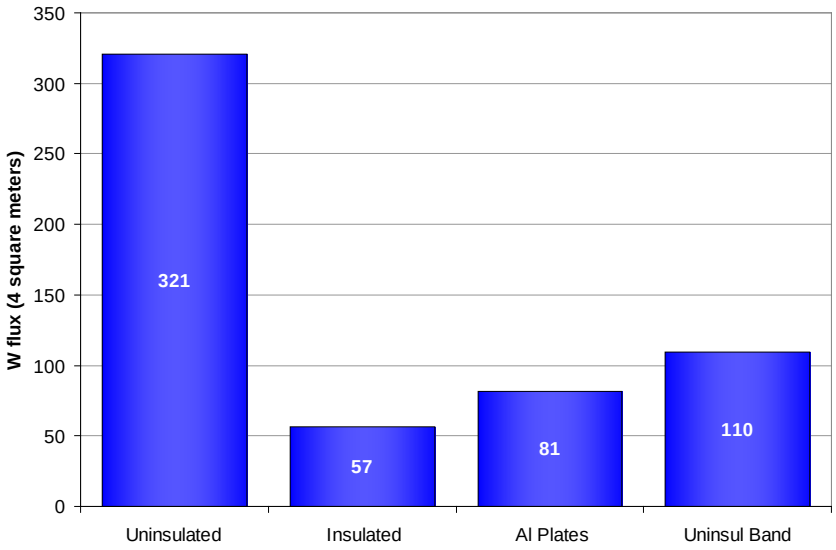

Figure 7: Heat loss through 42 sf (4 m^2) of wall assembly with joist framing, various cases

HYGROTHERMAL SIMULATIONS

The thermal behavior of embedded beam and joist ends is only one facet for durability analysis: their hygrothermal behavior (and most importantly, the wetting and drying of the beam end) is of greater interest. Therefore, one-dimensional hygrothermal simulations were run of various insulated and uninsulated scenarios, using IBP WUFI Version 5.1. This version adds the ability to have air sourced from interior or exterior conditions into a cavity within the assembly, which was used in the sensitivity analysis.

However, one limitation was the use of a one-dimensional simulation. The cross-section at the beam end is the same in insulated and non-insulated cases, in a one-dimensional simulation. Therefore, the thermal properties of the wood material inboard of the beam pocket were changed, in order to “force” beam pocket temperatures similar to the three-dimensional thermal simulations.

The first step was to develop a temperature index of the beam pocket temperatures, of the insulated and uninsulated cases. HEAT3 models were run at a series of outdoor temperatures, and the resulting beam pocket temperatures were recorded and plotted in Figure 8. Note that these are steady state simulations, and do not account for the thermal mass of the masonry. This graph shows that in the uninsulated case, the thermal resistance inboard of the beam pocket is roughly 40% of the total, and the beam pocket temperatures are close to halfway between indoor and outdoor temperatures. Then in the insulated case, the thermal resistance inboard of the beam pocket is roughly 89% of the total, and the beam pocket temperature is close to exterior

conditions.

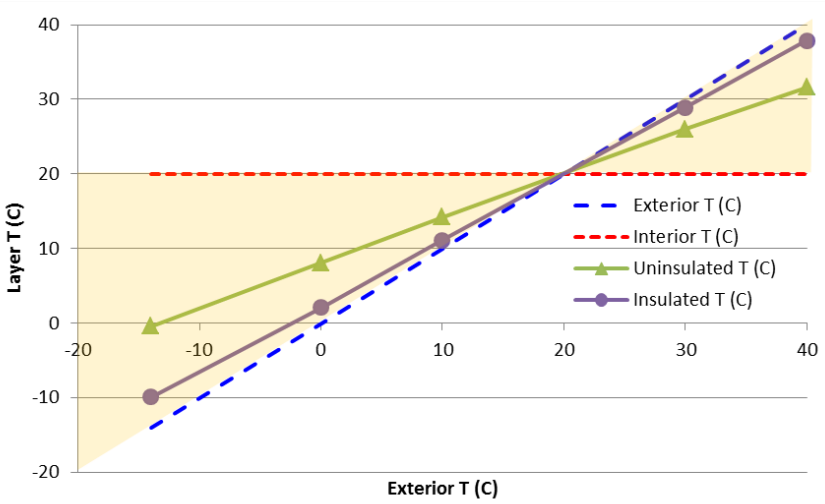

Figure 8: Temperature at end of beam for uninsulated and insulated cases

The one-dimensional hygrothermal simulations were then created to "force" these temperature differences; the approach was to calculate the relative thermal resistances inboard and outboard of the beam pocket air space, and to modify them as per the temperature index above. The initial dimensions and material chosen in the hygrothermal simulation resulted in thermal resistances close to the temperature index value (41% outboard/59% inboard), and were used as-is. In the insulated hygrothermal simulations, the thermal conductivity of the oak beam was changed from 0.043 Btu·in / (hr·ft^2·°F) or 0.3 W/m·K to 0.0072 Btu·in / (hr·ft^2·°F) or 0.05 W/m·K, resulting in an 11% outboard/89% inboard thermal resistance balance. Note that these calculations are based on the dry thermal conductivities of these materials; the moisture-dependent thermal conductivities were not used in these calculations. The remaining moisture properties were left as per the default values.

The simulated assembly is shown below in Figure 9, which includes a brick masonry exterior, an air space, and an oak interior (or oak modified as per above).

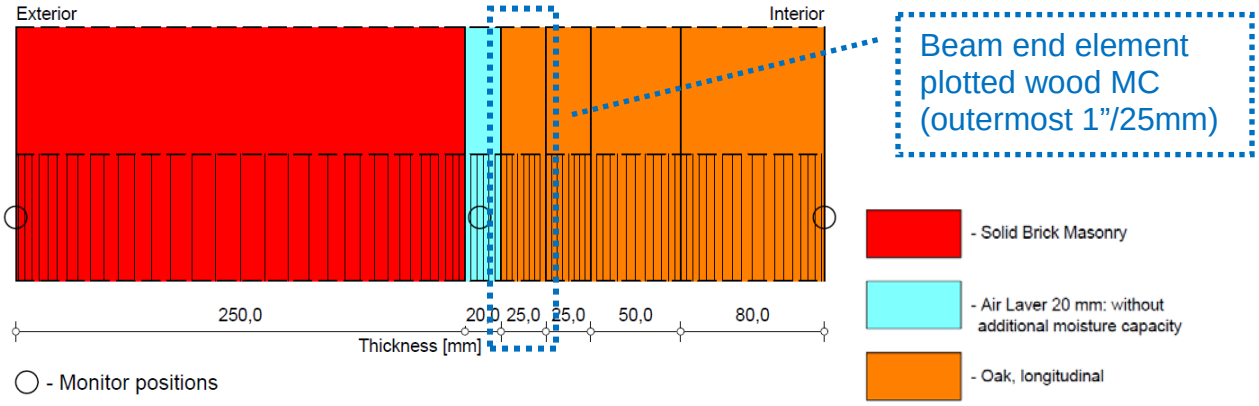

Figure 9: WUFI simulated assembly, showing components and dimensions

Simulations were run in a Boston (cold year) climate, facing northeast (worst driving rain orientation), for a period of three years. The interior conditions were 68° F/20° C constant temperature, with a sinusoidally varying relative humidity (30% winter to 60% summer).

In addition, in some cases, interior air was introduced into the air layer/beam pocket. In a typical existing installation, there is a noticeable gap around the beam, varying from roughly 1/8" to 1" (3-25 mm). The amount of air movement is unknown, so several bounding cases were simulated.

Simulations were run, and the wood moisture content of the outermost 1"/25mm of the wood beam was compared. The first cases were all uninsulated cases, with various amounts of airflow from the interior into the airspace: none, 10 air changes per hour (ACH), and 20 ACH.

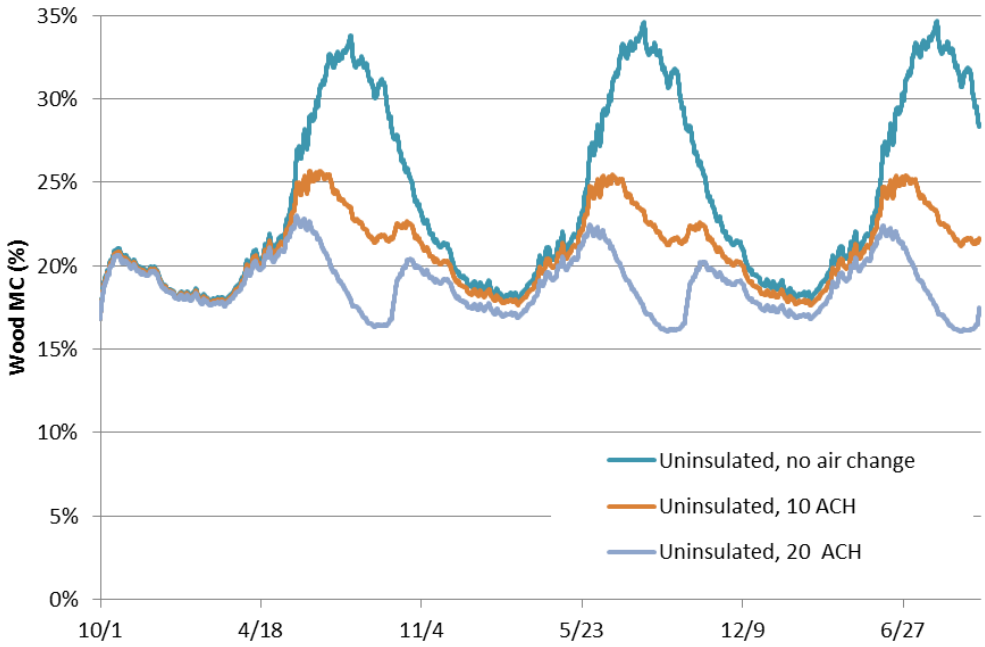

Figure 10: Wood beam end (1"/25 mm) moisture contents; uninsulated cases

Starting with the "no air change" case, it was noted that the spikes in moisture content do not occur during the winter, as might be expected, but instead in the summertime. This was due to rainwater absorption in the outer brick layers, which was then driven into the beam end by the inward temperature gradient. The addition of air change from the interior resulted in summertime drying, with greater drying from higher air change rates (10 ACH vs. 20 ACH). This drying effect also occurred in the wintertime: high wood moisture content due to condensation of interior air on the beam end was not observed in these simulations. However, this was with low (30% peak) wintertime interior RH conditions.

It was also noted that the moisture content spikes of the beam end in the "no air change" case were very high, at roughly 35% MC. Cycling to this level is unlikely in

reality, given the likelihood of moisture damage at these conditions. This suggests that air change with the interior might play a role in the drying of beams in existing buildings. However, these simulations do not take into account the three-dimensional aspects of the beam pocket, such as redistribution of moisture from the outer face of the beam to the remaining sides of the pocket.

The next sets of simulations examined the insulated cases, which created lower air space temperatures in wintertime by reducing the thermal conductivity through the wood elements. The resulting wood beam end moisture contents are shown in Figure 11. Surprisingly, the "no air change" case results in lower peak moisture contents in the beam end, albeit with a similar seasonal pattern to the uninsulated case. This could be due to the shift in relative thermal resistances: the majority of the thermal resistance (89%) is now inboard of the air pocket. Therefore, there is less temperature difference through the thickness of the masonry layer, resulting in less inward vapor drive.

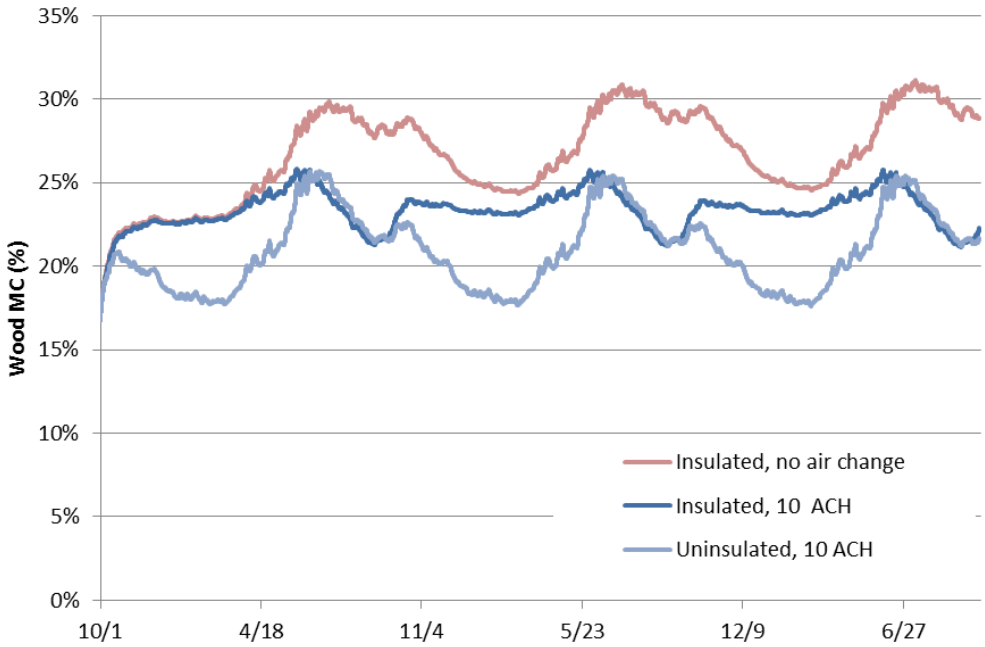

Figure 11: Wood beam end (1"/25 mm) moisture contents; insulated cases (+ uninsulated)

Again, the addition of air change results in reduced moisture accumulation at the beam end. The 10 ACH insulated and uninsulated cases are shown together for comparison: summertime wood moisture contents are largely identical. But in wintertime, the insulated case has higher moisture contents: this is reasonable, given the risks of condensation on interstitial surfaces that are now colder, due to interior insulation. Note that these simulations use a low wintertime relative humidity (30%); wintertime condensation issues would be substantially worse at higher interior RH levels.

The previous simulations use a monolithic exterior material ("Solid brick masonry"; IBP database), which is intended to simulate brick masonry (including mortar joints) as a composite material. Actual construction of mass masonry walls is composed of multiple wythes of brick, with incomplete infill. This results in some air spaces between layers,

and less than perfect capillary contact. To get some indication of the effect of changing the exterior materials, another set of simulations were run building up the exterior wall with multiple brick wythes and a layer of mortar, as per Figure 12. All other simulation characteristics were kept the same; for reference, the proportion of dry thermal resistances was 14% outboard/86% inboard, similar to previous cases.

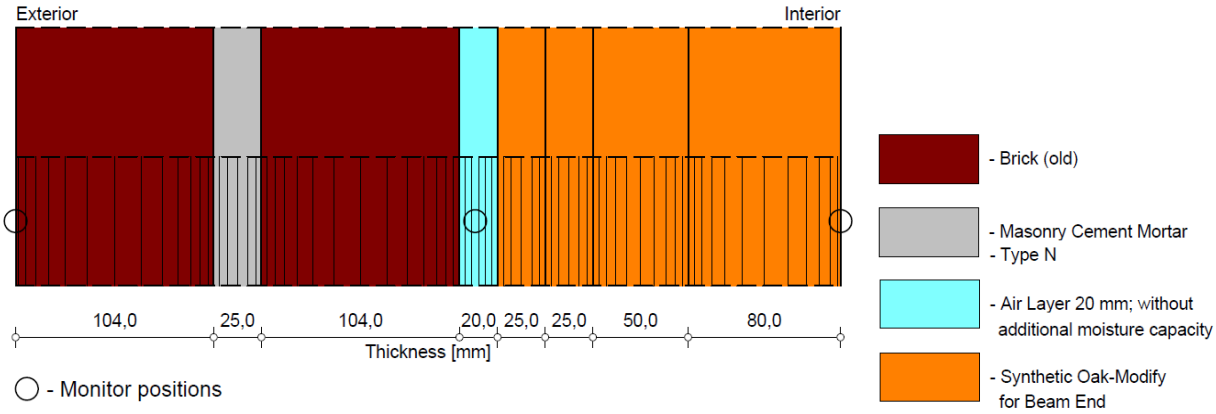

Figure 12: WUFI simulated assembly (components and dimensions), non-monolithic exterior

The resulting moisture contents at the end of the wood beam are shown below in Figure 13. All of the moisture content levels are markedly lower than previous simulations.

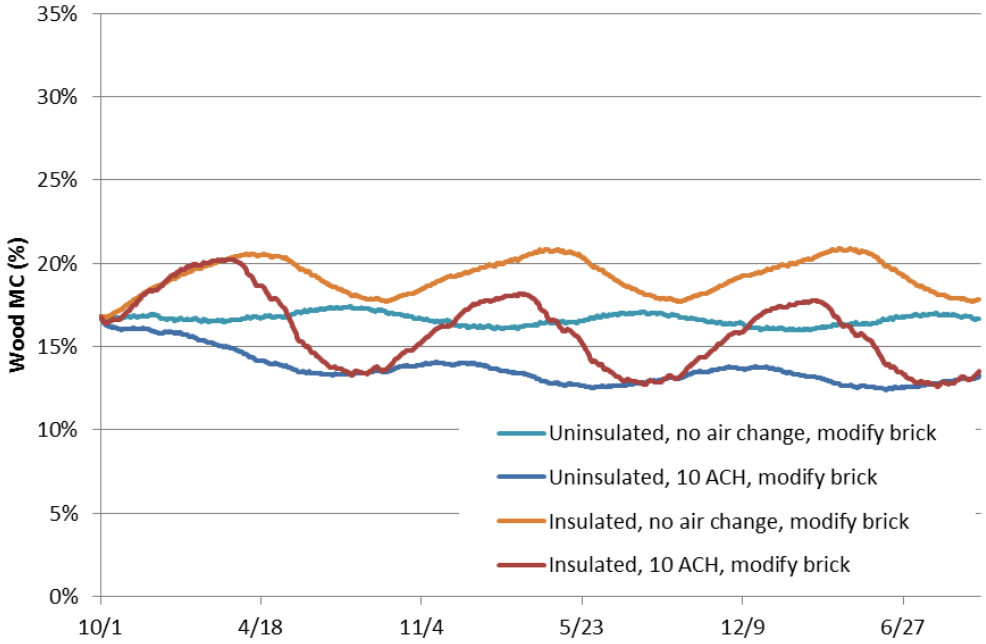

Figure 13: Wood beam end (1"/25 mm) moisture contents; modified exterior brick cases

General patterns of behavior are similar to previous cases though: the uninsulated (no air change) case has a sinusoidal pattern, but with moisture contents well within typical safe ranges. The addition of air change results in even lower moisture contents; however, the sinusoidal pattern reverses, with peaks in wintertime, which could be

ascribed to moisture accumulation on cold surfaces.

The addition of insulation results in elevated moisture contents compared to the uninsulated cases; peaks are seen in wintertime conditions, but levels peak only slightly above 20% MC (as opposed to 30%+). The addition of air change in the insulated case results in drier conditions at the beam end; moisture content peaks occur in the winter as well.

CONCLUSIONS AND FURTHER WORK

Three-dimensional static thermal simulations of large ("beams") and small ("joist") embedded wood members in masonry assemblies showed the expected patterns, of colder wintertime beam end temperatures after the retrofit of interior insulation. Various methods to allow greater heat flow were simulated, with the goal of raising wintertime beam end temperatures. The use of passive aluminum plates adjacent to the beams and joists showed a moderate increase in beam end temperatures, with some penalty in overall assembly heat flux. The analogous joist case showed higher beam end temperatures, but it seems unlikely to be executed in practice. The use of thinned (1" thick/25 mm vs. 2" thick/50 mm) insulation near beam ends showed little effect on beam end temperatures. The elimination of insulation at the rim joist area resulted in temperatures close to original conditions; however, static thermal simulations indicate that there might be significant risk of wintertime condensation within the cavities at typical interior humidity conditions. In addition, this measure loses a significant fraction of the energy savings of the fully insulated case (roughly double the heat loss).

The hygrothermal simulations rely on a modification of material properties (thermal conductivity), in order to run uninsulated and insulated cases in a one-dimensional model. The moisture content of the outermost 1"/25mm of the beam was plotted as a measure of relative performance. In addition, interior air was introduced into the air space between wood and masonry at various levels.

Simulations with initial assumptions showed that air leakage has a strong effect of wood moisture content: the uninsulated case showed summertime moisture peaks of almost 35%, which is unrealistic for sustained durability. Increasing air flow rates into the pocket resulted in lower moisture contents. The addition of insulation (with no air flow) resulted in wood moisture contents lower than the uninsulated (no air flow) cases; however, peaks were still in the 30% range. The addition of airflow lowered summertime moisture contents.

A final set of simulations were run using an exterior masonry assembly with different material properties, which resulted in markedly different beam end moisture contents. Uninsulated performance was in the 13-17% MC range, and insulated in the 13-21% range.

Overall, these simulations indicate that there is substantial uncertainty in how embedded wood members in masonry actually behave in service after insulation retrofits. The properties of the exterior masonry has a tremendous effect of the beam end moisture contents: not only material properties (e.g., liquid water uptake), but also

macroscopic effects (not simulated here) such as infill between brick wythes. The effect of airflow into the beam pocket can be significant, while actual air change rates are unknown. In addition, Morelli et al. (2010) demonstrated that rainwater exposure can have a tremendous effect on beam pocket relative humidity conditions. Finally, it is acknowledged that these one-dimensional hygrothermal simulations are a workaround for a complex three-dimensional problem.

These factors suggest that further research is warranted: at a minimum, the use of two-dimensional hygrothermal simulations, with more refined assumptions for air change rates. However, even these may prove to be of limited applicability, given the effect of material property assumptions. Ideally, in-situ measurements of beam pocket temperatures, relative humidity, and wood moisture content (in both insulated and uninsulated configurations, and various orientations and rainfall exposure levels) would provide the greatest insight into true behavior. The exposure conditions may prove to be one of the key factors, based on Dumont et al. (2005): liquid water loading such as capillarity from the ground, splashback from adjacent rainfall, or poor rain control detailing might provide crucial differences between success and failure.

One solution that is worth considering in interior insulation retrofit cases might be so-called “hygric diode” materials, as used in commercially available “wicking” (but vapor impermeable) pipe insulation. This would have the effect of removing liquid water condensation (were it to occur) from the masonry beam pocket, and drying it to the interior.

ACKNOWLEDGEMENTS

The authors would like to thank the US Department of Energy’s Building America Program for funding this research.

REFERENCES

Blomberg, T. 1996. “Heat Conduction in Two and Three Dimensions: Computer Modeling of Building Physics Applications.” Report TVBH-1008, Department of Building Physics, Lund University, Sweden.

Dumont, R., L. Snodgrass, J. Kokko, J. Goth, C. Schumacher. 2005. "Field Measurement of Wood Moisture Contents in Wood Joists Embedded in Masonry Exterior Walls." Proceedings of the 10th Annual Conference on Building Science and Technology. 2005. Ottawa, ON.

Gonçalves, M.D. 2003. "Insulating Solid Masonry Walls." Ninth Conference on Building Science and Technology, Ontario Building Envelope Council, Vancouver, BC, pp. 171-181.

Hutcheon, N.B. 1964. NRC-IRC (National Research Council of Canada-Institute for Research in Construction) Canadian Building Digest CBD-50. “Principles Applied to an Insulated Masonry Wall,” Ottawa, ON: National Research Council of Canada.

Mensinga, P., J. Straube, C. Schumacher, C., et.al. 2010. “Assessing the Freeze-Thaw

Resistance of Clay Brick for Interior Insulation Retrofit Projects” Performance of the Exterior Envelopes of Whole Buildings XI. Atlanta, GA: American Society of Heating, Refrigeration, and Air-Conditioning Engineers, Inc. Proceedings of Building XI Conference Clearwater, FL.

Morelli, M., G. Scheffler, T. Nielsen, S. Svendsen. 2010. “Internal Insulation of Masonry Walls with Wooden Floor Beams in Northern Humid Climate.” Performance of the Exterior Envelopes of Whole Buildings XI. Atlanta, GA: American Society of Heating, Refrigeration, and Air-Conditioning Engineers, Inc.

Nady M., A. Saïd, W. Brown, I. Walker. 1997. “Long-Term Field Monitoring of an EIFS Clad Wall” Journal of Thermal Insulation and Building Envelopes, Vol 20, April 1997, pp 320-338

Rousseau, M.Z., A.H.P. Maurenbrecher. 1990. ‘‘Rehabilitation of Solid Masonry Walls’’, Construction Practice Publication, Institute for Research in Construction (http://irc.nrc-cnrc.gc.ca /pubs/cp/wal1_e.html). Originally published in "Construction Canada" 32(5), 1990, p. 15-20

Scheffler, G.A. 2009. “Moisture Problems at Wooden Beam Ends after Building Renovation.” LavEByg konference om strategi for lavenergirenovering, 22. April 2009, Hørsholm, Denmark.

Straube, J.F., and Schumacher, C.J. 2002. "Comparison of Monitored and Modeled Envelope Performance for a Solid Masonry Building." CMHC Report, Ottawa, ON.

Straube, J.F., and Schumacher, C.J. 2004. "Hygrothermal Modeling of Building Envelopes Retrofits." CMHC Report, Ottawa, ON.